



Numerical Modelling of the Creep Subsidence of an Ocean Lighthouse Constructed on a Reclaimed Coral Reef Island

Dawei Yu^{a,b} and Jianhong Ye^a

^aInstitute of Rock and Soil Mechanics, Chinese Academy of Sciences, Wuhan 430071, China

^bSchool of Engineering and Technology, China University of Geosciences (Beijing), Beijing 100083, China

ARTICLE HISTORY

Received 4 March 2020
Revised 11 August 2020
Accepted 1 December 2020
Published Online 10 February 2021

KEYWORDS

Modified Burgers creep model
Calcareous coral sand foundation
Long-term creep subsidence
Ocean lighthouse
Creep behavior
Coral reef
South China Sea

ABSTRACT

This work is to investigate the creep subsidence of a large-scale ocean lighthouse constructed on a reclaimed calcareous coral sand foundation (abbreviated to RCCSF thereafter) in the South China Sea (SCS). Firstly, two modified Burgers creep models, referred to as modified HBM and KBM, respectively, are proposed and validated based on several triaxial creep test results, and then both are implanted into ABAQUS. Secondly, the model parameters of the modified Huang's Burgers Creep Model (HBM) and Kong's Burgers Creep Model (KBM) for the RCCSF are carefully calibrated for the subsequent numerical modelling according to the creep tests conducted by us. Thirdly, based on the modified HBM and KBM proposed in this study and the calibrated model parameters, the subsidence of an ocean lighthouse constructed on a reclaimed land in the South China Sea is numerically analyzed. The numerically predicted results illustrate that the creep subsidence of the ocean lighthouse in the future 50-year is 17.2 mm to 42.5 mm, meeting the mandatory requirement (<200 mm) stipulated by the China national design code. Finally, the sensitivity of the predicted creep subsidence to the model parameters is screened by performing parametric analysis.

1. Introduction

Coral reef is kind of mountain in ocean formed due to the deposition and cementation of marine creature's organic skeletons in the geologic history. It mainly develops in the tropical ocean environment, and is widely distributed in the tropical water between 30° south latitude and 30° north latitude. Calcareous coral sand (abbreviated to CCS thereafter) is a type of ocean deposit generally located on the top platform of the coral reefs, mainly consists of the fragments and gravels of marine organism skeletons. CCS has the special mechanical properties of high porosity, fragility, high compressibility and relatively poor hardness. It is highly crushable when applied by a middle to high stress. As a result, the engineering properties of CCS foundation are significantly different with the terrestrial quartzose and siliceous sands, or other types of marine deposits. These special engineering properties of CCS bring a great challenge to geotechnical engineers involved in design in recent decades, due to the fact that the traditional methods and engineering experiences based on terrestrial soil foundations are not effective for the CCS foundation.

Therefore, special attention should be paid on the characteristics of CCS when conducting engineering activities on coral reefs.

Lighthouses constructed on reclaimed coral reef islands are important for navigation safety, maritime rescue and fishery production. Since 2015, five large lighthouses with a height of about 60 meters have been successfully constructed on the RCCSF in the SCS, filling the blank of civil navigation aid facilities in the area. The creep behavior of the lighthouses foundation has attracted the attention of coastal engineers in design process, because the excessive long-term creep subsidence would cause the lighthouse to lose their normal service ability. Therefore, the prediction of the post-construction creep subsidence of the ocean lighthouses is a crucial issue.

A series of creep mathematical models of soils actually have been proposed based on creep experimental data to quantitatively investigate the long-term subsidence of structures, for example, Nishihara creep model (Nishihara, 1952, 1958), Singh and Mitchell creep model (Singh and Mitchell, 1968), Burgers creep model (Dorfman and Faller, 1982), Mesri creep model (Mesri et al., 1981), and Murayama creep model (Murayama, 1983) etc.. In

recent two decades, He et al. (2011) and Fu and Huang (2008) respectively modified the classical Burgers model into new forms. We call them as Huang's Burgers model (HBM) and Kong's Burgers model (KBM), respectively in this study. Among them, HBM introduced an exponential function into the classic Burgers model, while KBM changed the power of time term in the original Burgers model from 1 to a decimals.

The aforementioned studies are all about creep mathematical models, creep testing is also an important way to investigate the creep deformation of materials. Lv et al. (2017) investigated comparatively the creep characteristics of quartz sand and CCS through some triaxial creep tests. It was shown by their results that the axial creep strain of CCS could be 20 times of that of quartz sand; and the volumetric creep could be 5 times of quartz sand. Based on a number of creep experiments, Enomoto et al. (2016) studied the creep characteristics of gravel soil. Recently, Cao and Ye (2019) and Ye and Cao (2019) conducts a number of creep experiments for the coral sand from the SCS. Cao and Ye (2019) further establishes a nonlinear equation between the initial elastoplastic strain ε_0 and the confining pressure p , as well as the applied deviatoric stress q based on their experimental data.

So far, there are usually two type of method for determining the long-term creep subsidence of structures. They are numerical simulation and field monitoring (Jiang and Lin, 2010; Shen et al., 2014, Di et al., 2016; Shi et al., 2018), respectively. However, the method of field monitoring is difficult to be continuous for more than 10 years and the cost would be very expensive. Therefore, if the monitoring period for the post-construction settlement of structures exceeds ten years, the numerical method may be more appropriate. So far as we know, many researchers have conducted a great number of research works on the numerical method to predict the creep deformation of soil foundation, as well as the resulting creep subsidence of structures, for example, Pramthawee et al. (2017), Zhang et al. (2018a), Qiu et al. (2018), Zhang et al. (2018c), Wongsaroj et al. (2013), Yao et al. (2019).

Since 2015, five large ocean lighthouses have been successfully constructed on the newly RCCSF in the SCS. Generally, the newly RCCSF is loose relative to the naturally deposited sand foundation which has experienced a long term consolidation in the geological history (Wang et al., 2009; Shahnazari and Rezvani, 2013). Therefore, the creep-induced subsidence of these lighthouses should be paid serious attention and should be quantitatively predicted. So far as we know, there is no a

literature is available to study the post-construction creep subsidence of the lighthouses constructed on the newly RCCSF in the SCS employing numerical method. In this study, two modified creep models HBM and KBM are proposed and validated based on several triaxial creep results, and both are embedded into ABAQUS firstly. Secondly, the model parameters of the modified HBM and KBM for the calcareous sand foundation of these lighthouses are carefully calibrated for the following numerical prediction. Finally, adopting the modified HBM and KBM proposed by us and the calibrated model parameters, the long-term post-construction creep subsidence of an ocean lighthouse constructed on a RCCSF in the SCS is predicted.

2. Creep Model

In previous studies, a series of creep constitutive models have been proposed, for example, Nishihara model, Singh and Mitchell model, Burgers model, etc. Among them, the Burgers model is widely applied to predict the creep subsidence of structures. In the following, two modified Burgers creep models will be established for the CCS coming from SCS based on the results of several triaxial creep tests.

2.1 Kong's Burgers Creep Model (KBM)

The original Burgers creep model was modified by He et al. (2011) into a new form, referred to as KBM here, according to the elements setup as illustrated in Fig. 1(a).

The KBM is expressed as

$$\varepsilon = \frac{q}{E_0} + \frac{q}{E_1} (1 - e^{-R}) + \frac{q}{C} t^\beta, \tag{1}$$

where q is the deviatoric stress, ε is the total strain. E_0 is the deformation modulus of material; $R = E_1/\eta_1$, in which η_1 is the coefficient of viscosity. $C = \xi\Gamma(1+\xi)$, in which ξ and β are the parameters characterizing the soft body element. It is noticed that the creep deformation determined by the KBM will not be converged with time. But the growth rate of the creep deformation will be quite slow in the later period of creep.

2.2 Huang's Burgers Creep Model (HBM)

The creep strain predicted by the KBM does not converge with time. To overcome this problem, Fu and Huang (2008) established a converged Burgers model, referred to as HBM, according to the elements setup as illustrated in Fig. 1(b).

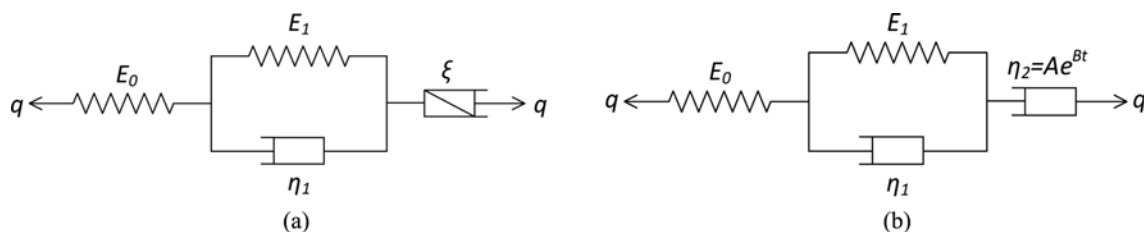


Fig. 1. Schematic Diagrams of KBM and HBM: (a) KBM, (b) HBM

The HBM is expressed as

$$\varepsilon = \frac{q}{E_0} + \frac{q}{E_1}(1 - e^{-\tau}) + \frac{q}{AB}(1 - e^{-B}), \quad (2)$$

where the parameters A and B are used to characterize the dashpot, $\tau = E_1/\eta_1$. In Eq. (2), it is found that the creep deformation determined by HBM will be converged with time due to the introduction of two exponential functions.

2.3 Modified Burgers Creep Model

The parameter E_0 in Eqs. (1) and (2) is actually a constant. But, previous literatures (Cao et al., 2017; Zhang et al., 2018b) have clearly demonstrated the fact that E_0 is related to p and q . The above KBM and HBM will be further modified based on this recognition in this section.

Cao and Ye (2019) conducted a number of laboratory triaxial creep tests for the CCS sampled from the SCS. Based on the experimental results, they established a nonlinear relationship between ε_0 , q and p :

$$\varepsilon_0 = K \frac{(q/P_a)^m}{(p/P_a)^n}, \quad (3)$$

where ε_0 is initial elastoplastic strain, p is the effective confining pressure, q is the deviatoric stress. P_a is the one standard atmosphere (101.3 kPa), playing the role of dimensionless. K , n and m are three dimensionless parameters related to soil property. As illustrated in Fig. 2, ε_0 has a linear relationship with $(q/P_a)^m/(p/P_a)^n$. It can be seen that the R^2 both are greater than 0.92, regardless of the dry density.

Based on the Eq. (3) and the constitutive relation $q = E_0\varepsilon_0$, the equation between E_0 , p and q can be expressed as

$$\frac{q}{\varepsilon_0} = E_0 = \frac{q}{K} \frac{(p/P_a)^n}{(q/P_a)^m}. \quad (4)$$

Then combining Eqs. (4) and (1), the modified KBM is expressed as

$$\varepsilon = K \frac{(q/P_a)^m}{(p/P_a)^n} + \frac{q}{E_1} \left(1 - e^{-\frac{E_1}{\eta_1}} \right) + \frac{q}{C} t^\beta, \quad (5)$$

and combining Eqs. (4) and (2), the modified HBM can be expressed as

$$\varepsilon = K \frac{(q/P_a)^m}{(p/P_a)^n} + \frac{q}{E_1} \left(1 - e^{-\frac{E_1}{\eta_1}} \right) + \frac{q}{AB} (1 - e^{-B}). \quad (6)$$

2.4 Finite Element Implementation

The creep strain in Eqs. (5) and (6) actually is formulated based on 1D stress condition. But, the stress condition in a real structure's foundation is 3D in the modelling of the creep behavior of soil foundation. Therefore, building a connection between Eqs. (5), (6) and the 3D stress condition is necessary to make sure that Eqs. (5) and (6) can be applied in 2D/3D numerical modelling. Fu and Huang (2008) have built this connection through extending the classic plastic theory to creep analysis.

Firstly, it is assumed that flow law and associated yield criterion are still applicable in the creep stress-strain relationship. The differential form of creep strain $d\varepsilon_{ij}^c$ is expressed as

$$d\varepsilon_{ij}^c = \lambda_c \left(\frac{\partial f}{\partial \sigma_{ij}} \right) dt \quad \text{and} \quad \frac{\partial f}{\partial \sigma_{ij}} = S_{ij}, \quad (7)$$

where λ_c is a scalar, f is the loading surface similar to that in plastic theory, S_{ij} is the deviatoric stress tensor. Writing the above Eq. (7) into the form of rate:

$$\frac{d\varepsilon_{ij}^c}{dt} = \dot{\varepsilon}_{ij}^c = \lambda_c \left(\frac{\partial f}{\partial \sigma_{ij}} \right). \quad (8)$$

According to the Von Mises theory, the differential equivalent creep strain $d\bar{\varepsilon}^c$ and the equivalent deviatoric stress of Von Mises $\bar{\sigma}$ can be written as

$$d\bar{\varepsilon}^c = \left(\frac{2}{3} d\varepsilon_{ij}^c d\varepsilon_{ij}^c \right)^{\frac{1}{2}} \quad \text{and} \quad \bar{\sigma} = \left(\frac{3}{2} S_{ij} S_{ij} \right)^{\frac{1}{2}}. \quad (9)$$

Combing the Eqs. (8) and (9), the rate of the equivalent creep

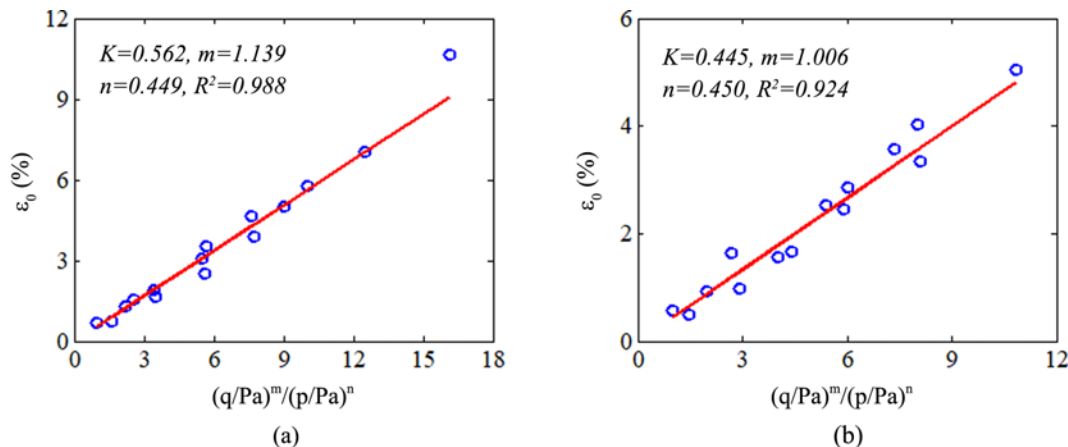


Fig. 2. Relationship between ε_0 and q, p for the Calcareous Sand From the SCS (Ye and Cao, 2019): (a) $\rho_d = 1.45 \text{ g/cm}^3$, (b) $\rho_d = 1.65 \text{ g/cm}^3$

strain is

$$\dot{\bar{\varepsilon}}^c = \frac{d\bar{\varepsilon}^c}{dt} = \left(\frac{2}{3} \frac{d\varepsilon_{ij}^c}{dt} \frac{d\varepsilon_{ij}^c}{dt} \right)^{\frac{1}{2}} = \left(\frac{2}{3} \dot{\varepsilon}_{ij}^c \dot{\varepsilon}_{ij}^c \right)^{\frac{1}{2}} = \lambda_c \left(\frac{2}{3} \frac{\partial f}{\partial \sigma_{ij}} \frac{\partial f}{\partial \sigma_{ij}} \right)^{\frac{1}{2}} = \frac{2}{3} \lambda_c \bar{\sigma}. \quad (10)$$

Then the scalar λ_c is determined as

$$\lambda_c = \frac{3 \dot{\bar{\varepsilon}}^c}{2 \bar{\sigma}}. \quad (11)$$

Finally, substituting Eq. (11) into Eq. (7), the differential creep strain under the Von Mises criterion becomes

$$d\varepsilon_{ij}^c = \frac{3 \dot{\bar{\varepsilon}}^c}{2 \bar{\sigma}} S_{ij} dt. \quad (12)$$

Then the incremental creep strain from time t to $t + \Delta t$ in one time step can be obtained through the following integration

$$\Delta \varepsilon_{ij}^c = \int_t^{t+\Delta t} d\varepsilon_{ij}^c = \int_t^{t+\Delta t} \frac{3 \dot{\bar{\varepsilon}}^c}{2 \bar{\sigma}} S_{ij} dt. \quad (13)$$

According to Eqs. (5) and (6), the rate of the equivalent creep strain $\dot{\bar{\varepsilon}}^c$ at time t and $t + \Delta t$ in Eq. (14) can be determined through time derivative:

$$\dot{\bar{\varepsilon}}^c = \frac{\bar{\sigma} \beta}{C} t^{(\beta-1)} + \frac{\bar{\sigma}}{\eta_1} e^{-E_1 t / \eta_1}, \quad \text{and} \quad \dot{\bar{\varepsilon}}^c = \frac{\bar{\sigma} \beta}{C} (t+\Delta t)^{(\beta-1)} + \frac{\bar{\sigma}}{\eta_1} e^{-E_1 (t+\Delta t) / \eta_1}, \quad (14)$$

for the modified KBM; and

$$\dot{\bar{\varepsilon}}^c = \frac{\bar{\sigma}}{A} e^{-Bt} + \frac{\bar{\sigma}}{\eta_1} e^{-E_1 t / \eta_1}, \quad \text{and} \quad \dot{\bar{\varepsilon}}^c = \frac{\bar{\sigma}}{A} e^{-B(t+\Delta t)} + \frac{\bar{\sigma}}{\eta_1} e^{-E_1 (t+\Delta t) / \eta_1}, \quad (15)$$

for the modified HBM. Due to the fact that the rate of the equivalent creep strain $\dot{\bar{\varepsilon}}^c$, the equivalent deviatoric stress of Von Mises $\bar{\sigma}$, and the deviatoric stress tensor S_{ij} are all function of time in creep process, the integration in Eq. (13) is nonlinear. Generally, the generalized central point method of implicit integration is used to determine the integral value $\Delta \varepsilon_{ij}^c$. The corresponding iterative formulation of Eq. (13) is

$$\Delta \varepsilon_{ij}^c = \frac{3}{2} \frac{t+\theta \Delta t}{t+\theta \Delta t} \frac{\dot{\bar{\varepsilon}}^c_{(k)}}{\bar{\sigma}_{(k)}} \Delta t S_{ij(k)} \quad (k=0, 1, 2, 3, \dots), \quad (16)$$

k is the symbol indicating the iterative times. Among them,

$${}^{t+\theta \Delta t} \dot{\bar{\varepsilon}}^c_{(k)} = (1-\theta) {}^t \dot{\bar{\varepsilon}}^c + \theta {}^{t+\Delta t} \dot{\bar{\varepsilon}}^c_{(k)}, \quad (17)$$

$${}^{t+\theta \Delta t} \bar{\sigma}_{(k)} = (1-\theta) {}^t \bar{\sigma} + \theta {}^{t+\Delta t} \bar{\sigma}_{(k)}, \quad (18)$$

$${}^{t+\theta \Delta t} S_{ij(k)} = (1-\theta) {}^t S_{ij} + \theta {}^{t+\Delta t} S_{ij(k)}, \quad (19)$$

where $0 \leq \theta \leq 1$. When $\theta \geq 1/2$, the above implicit integration scheme is stable. In the $(k+1)$ th iteration, once the incremental creep strain $\Delta \varepsilon_{ij}^c$ is determined, then the incremental elastic strain $\Delta \varepsilon_{ij}^{elastic}$ can be determined by the following equation:

$$\Delta \varepsilon_{ij}^{elastic} = \Delta \varepsilon_{ij} - \Delta \varepsilon_{ij}^c, \quad (20)$$

where $\Delta \varepsilon_{ij} = \frac{1}{2} (\Delta u_{i,j} + \Delta u_{j,i})$ is the total strain. Finally, the incremental stress $\Delta \sigma_{ij}$ and the updated stress at time $t + \Delta t$ can be determined by the following Eqs. (21) and (22):

$$\Delta \sigma_{ij} = D_{ijmn}^c \Delta \varepsilon_{nm}^{elastic}, \quad (21)$$

$${}^{t+\Delta t} \sigma_{ij} = {}^t \sigma_{ij} + \Delta \sigma_{ij}, \quad (22)$$

in which D_{ijmn}^c is the elastic matrix, expressed as

$$D_{ijmn}^c = \begin{Bmatrix} \lambda + 2G & \lambda & \lambda & 0 & 0 & 0 \\ \lambda & \lambda + 2G & \lambda & 0 & 0 & 0 \\ \lambda & \lambda & \lambda + 2G & 0 & 0 & 0 \\ 0 & 0 & 0 & G & 0 & 0 \\ 0 & 0 & 0 & 0 & G & 0 \\ 0 & 0 & 0 & 0 & 0 & G \end{Bmatrix}, \quad (23)$$

where λ, G are elastic parameter of soil, determined by Eq. (24):

$$\lambda = \frac{E_0 \mu}{(1-2\mu)(1+\mu)}, \quad G = \frac{E_0}{2(1+\mu)}, \quad K = \frac{E_0}{3(1-2\mu)}, \quad (24)$$

$$E_0 = \frac{q}{K} \left(\frac{p}{P_a} \right)^n \left(\frac{q}{P_a} \right)^m,$$

in which μ is Poisson's ratio, G is shear modulus. E_0 is the deformation modulus of soil. Its expression is coming from Eq. (4).

When the incremental creep strain at $(k+1)$ th iteration and at previous k th iteration satisfies the relation $\frac{\|\Delta \varepsilon_{ij}^c_{(k+1)} - \Delta \varepsilon_{ij}^c_{(k)}\|}{\|\Delta \varepsilon_{ij}^c_{(k)}\|} \leq err$,

it means the iteration at the current time step t to $t + \Delta t$ is converged. As a result, the computation gets into the next time step. Otherwise, the iteration at the current time step t to $t + \Delta t$ will be continued, getting into the next iteration until the above mentioned convergence criterion is satisfied. The iterative algorithm in each time step is illustrated in Fig. 3.

The modified KBM and modified HBM are integrated into ABAQUS using the UMAT subroutine. The integrated process is as shown in Fig. 3. The modified KBM and modified HBM have considered the effect of p and q on E_0 . Therefore, E_0 at different position is not a fixed value, but is determined based on p and q . When involving the case of high ground stress, the treatment way of E_0 in this study is more appropriate.

3. Verification

Cao and Ye (2019), Ye and Cao (2019) conducted a number of laboratory triaxial creep experiments for the CCS from the in-site engineering field of one reclaimed land in the SCS. In this section, the modified KBM and modified HBM proposed are verified based on the experimental results provided by Cao and Ye (2019).

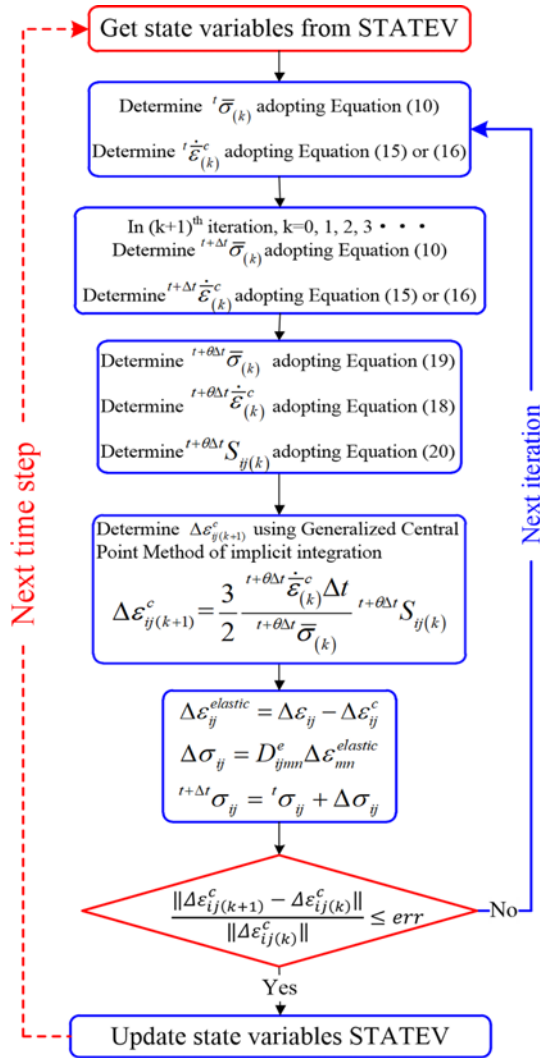


Fig. 3. The Flow Chart of Iterative Algorithm of the UMAT Subroutine in ABAQUS

A 3D cylindrical model is established at first. The size of model is consistent with the calcareous sand specimens in triaxial creep experiment. The radius and the height set as 30.9 mm and 120 mm, respectively. C3D8 element is used to mesh the model and the mesh size is 4 mm. The number of elements is 8,400 and the

Table 1. Stress Condition in the Triaxial Creep Experiment

ρ_d (g/cm ³)	p (kPa)	q (kPa)			
1.45	100	200	300	450	600
1.65	400	500	1,000	1,500	2,000

Note: ρ_d : dry density, q : deviatoric stress, p : confining pressure

number of nodes is 9,486 in total. The displacements in the x, y, and z direction on the bottom face of the model are all fixed. The modified KBM and modified HBM are used to determine the creep strain of the calcareous sand specimens. The applied stress condition in numerical computation is the same as that in the triaxial creep tests (Cao and Ye, 2019), that have been listed in Table 1.

The model parameters of the modified KBM and modified HBM should be determined before starting the verification work. According to the test results of the creep strain-time relationship provided by Cao and Ye (2019), the model parameters of the modified KBM and modified HBM can be determined through mathematical fitting. The parameters have been listed in Tables 2 and 3.

The predicted values of the creep strain determined by the modified KBM or modified HBM through ABAQUS and the experimental data (Cao and Ye, 2019) are both illustrated in Fig. 4. It can be observed that the numerical results are consistent with the triaxial creep tests results. It is indicated by this verification that the modified KBM and modified HBM established in this study are feasible and reliable to determine the creep subsidence of the RCCSF in the SCS.

4. Engineering Application

4.1 Engineering Background

So far, there are five large ocean lighthouses with a height of about 60 meters have been built on the reclaimed lands in the South China Sea. In this section, one of the lighthouses is chosen as the representative to study its post-construction settlement induced by the creeping of foundation soil by performing numerical analysis. To obtain the geological layers distribution, field drilling has been conducted on the RCCSF of the lighthouse

Table 2. Model Parameters of the Modified KBM Utilized in Computation

ρ_d (g/cm ³)	p (kPa)	q (kPa)	E_1 (MPa)	η_1 (GPa · min)	C (MPa)	β	K	m	n
1.45	100	200	315	13.9	499	0.1474	0.562	1.139	0.449
		300	345	32.7	443	0.1394			
		450	299	12.8	637	0.1522			
		600	189	6.44	616	0.1616			
1.65	400	500	1,079	93.9	2,520	0.1638	0.445	1.1006	0.45
		1,000	732	63	1,920	0.1841			
		1,500	958	79.2	2,140	0.1749			
		2,000	1,390	196	1,950	0.1963			

Table 3. Model Parameters of the Modified HBM Utilized in Computation

ρ_d (g/cm ³)	p (kPa)	q (kPa)	E_1 (MPa)	η_1 (GPa · min)	A (GPa)	B	K	m	n
1.45	100	200	274	624	4.6	0.0343	0.562	1.139	0.449
		300	235	302	6.5	0.0311			
		450	317	653	5.0	0.036			
		600	309	536	25	0.0416			
1.65	400	500	978	4,080	54.5	0.0128	0.445	1.1006	0.45
		1,000	663	2,780	62.9	0.0074			
		1,500	738	2,841	73.5	0.0193			
		2,000	470	1,590	24.2	0.0237			

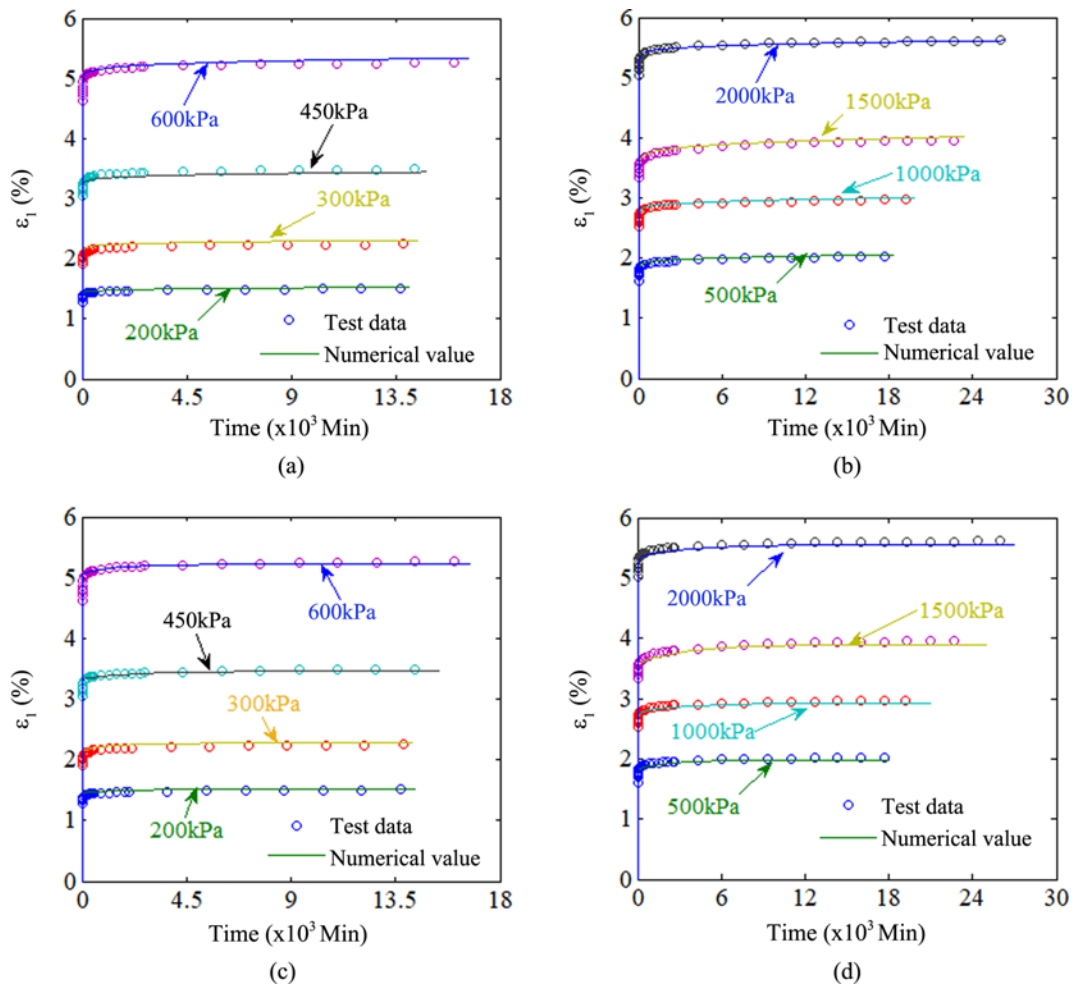


Fig. 4. Comparison between the Predicted Results and the Experimental Data (Cao and Ye, 2019; Ye and Cao, 2019): (a) $\rho_d = 1.45 \text{ g/cm}^3, p = 100 \text{ kPa}$ (KBM), (b) $\rho_d = 1.65 \text{ g/cm}^3, p = 400 \text{ kPa}$ (KBM), (c) $\rho_d = 1.45 \text{ g/cm}^3, p = 100 \text{ kPa}$ (HBM), (d) $\rho_d = 1.65 \text{ g/cm}^3, p = 400 \text{ kPa}$ (HBM)

in the SCS. There are totally about 30 boreholes with a depth 30 to 200 m have been completed in the lighthouse foundation. The typical photos are illustrated in Table 4. The drilling data shows that lighthouse foundation in the SCS consists of about three geological layers. The first soil layer is composed of the reclaimed loose CCS and its thickness is about 6 m. The second soil layer consists of the naturally deposited original calcareous sand. Its density is slightly denser than the first layer, and the thickness is

about 30 m. The third layer is the reef limestone if the buried depth $\geq 36 \text{ m}$. Compared with the overlying CCS, the reef limestone is much harder (uniaxial compressive strength is greater than 20 MPa). Therefore, creep strain of the coral reef limestone will be apparently small. As a consequence, the creep settlement of the lighthouse is mainly dependent on the creep deformation of the overlying reclaimed and original CCS. Based on this recognition, only the creep deformation of the above two layers (total 36 m)

Table 4. Typical Pictures and Brief Descriptions of the Drilling Samples for the Lighthouse's Coral Calcareous Sand Foundation

Photos of the drilling cores	Core depth (m)	State descriptions
	1 – 5	Creamy yellow; soil is in loose state, mainly composed of calcareous sands; sand particles are poorly graded; the content of coral gravels is less than 5%, which are primarily consisted of calcareous bioclastic detritus; containing a staghorn coral, 5 cm in length.
	6 – 10	Off-white; soil is medium dense state; consisting of coarse sand (original coral calcareous sand); soil particles are inhomogeneous, and poorly graded; the content of coral gravels and coral fragments is less than 5%, particle size is 1 – 5 cm.
	11 – 15	Off-white; mainly composed of original coral calcareous sands; soil particles are inhomogeneous and poorly sorted; the content of coral gravels and coral fragments is less than 5%; containing a coarse gravel, particle size is about 8 cm.
	16 – 20	Creamy yellow; soil is mainly in medium dense state; primarily composed of coarse sand; soil particles are inhomogeneous, and poorly graded; the content of coral gravels and coral fragments is less than 10%, particle size is 1 – 8 cm.
	21 – 25	Off-white; mainly composed of coarse sand; sand particles are inhomogeneous; containing a small amount of coral gravels; containing six coarse gravels, particle size is 5 – 8 cm.
	36 – 40	Coral reef limestone; lime white; The texture is hard; cores partially are fragments, and partially are short columns with a length 5 – 15 cm; partially are intercalated gravel limestone; the surface of the cores contains some original holes in these cores.

Note: The ground surface is as the zero elevation.

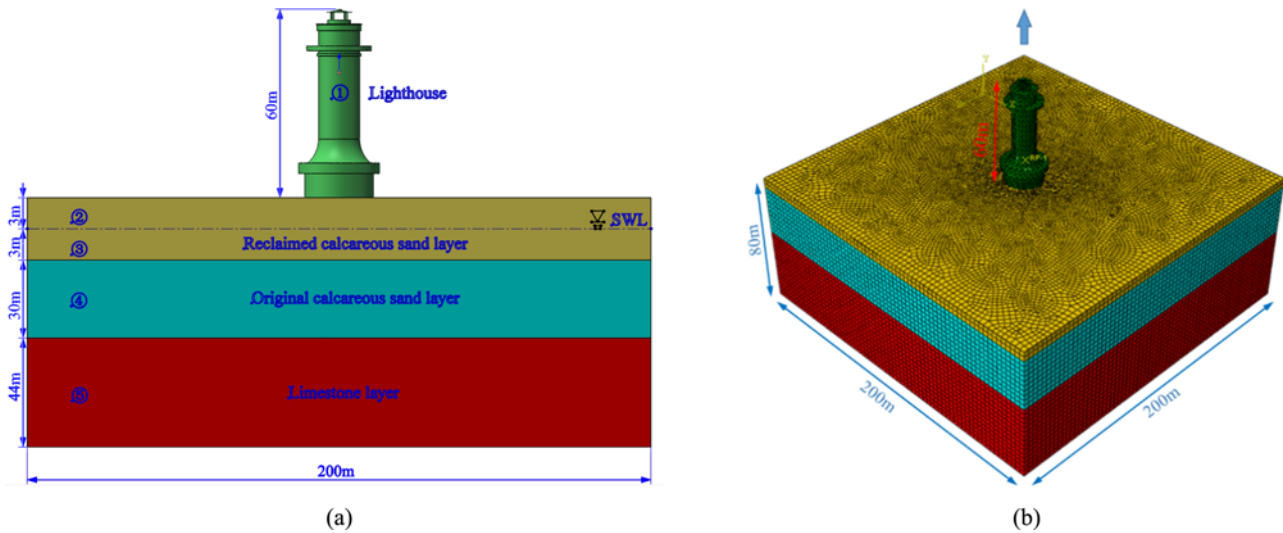


Fig. 5. 3D Geometry Model and the Mesh Generated for the Lighthouse and Its RCCSF in the SCS: (a) Schematic Diagram of Geometry Model, (b) Schematic Diagram of Mesh Generation

are considered when predicting the creep settlement of the lighthouse constructed on the RCCSF adopting the modified KBM and modified HBM.

4.2 Geometrical Model and Model Parameters

The schematic diagrams of the geometrical model is shown in Fig. 5. A lighthouse with a diameter 20 m and a height 60 m is constructed on RCCSF. The thickness of lighthouse foundation in the computational model is 80 m. In order to eliminate the effect of the fixed boundaries, the length and width of the lighthouse foundation is set as 200 m. The horizontal displacement of four lateral faces of the computational model are fixed; and the horizontal and vertical displacement of the bottom face of the model is fixed.

The dry density of the lighthouse foundation have been estimated at field through the drilling samples. The dry density of the first layer (total 6 m thick), second layer (total 30 m thick) and third layer (total 44 m thick) is about 1.45 g/cm³, 1.65 g/cm³ and 2.0 g/cm³, respectively. Through analyzing the observation data of water level line (SWL) in the past 3 years, it is found that the SWL in the lighthouse foundation varies from 2.5 m to 3.5 m below the ground surface during one year. Therefore, the SWL is taken 3 m in this study. The dry density is used above SWL and the floating density is used below SWL in numerical computation. Finally, the computational geometrical model is composed of five types of materials. They are the lighthouse, labelled as ①; the RCCSF over SWL, labelled as ②; the RCCSF beneath SWL, labelled as ③; the original calcareous sand, labelled as ④; and finally the limestone, labelled as ⑤. The lighthouse and reef limestone are both treated as elastic material. The elastic modulus of the lighthouse and reef limestone is set as 10 GPa and 13 GPa, respectively. The properties of the five materials are illustrated in Table 5.

The lighthouse is meshed using C3D10 element, which consists of 12,331 elements and 24,021 nodes. The lighthouse foundation

Table 5. Parameters of the Lighthouse and Foundation Used in Numerical Simulation

Materials	ρ_d (g/cm ³)	ρ_b (g/cm ³)	ν	e
①	2.8	2.8	0.2	0
②	1.45	1.45	0.28	0.96
③	1.45	0.939	0.28	0.96
④	1.65	1.123	0.3	0.9
⑤	2	1	0.2	0

Note: ν : Poisson's ratio; e : Void ratio. Materials ① is concrete, materials ⑤ is the reef limestone. Their void ratio are assumed as 0. The void ratio is calculated using formula $e = G_s \rho_w / \rho_d - 1$, where G_s is the relative density, $G_s = 2.83$ for calcareous coral sand (Liu et al., 1999). The buoyant density is calculated using the formula $\rho_b = \rho_d - \rho_w / (1 + e)$.

is meshed by C3D8 element, which consists of 402,539 elements and 414,308 nodes. Based on the modified KBM and the modified HBM, the creep deformation of the lighthouse constructed on the RCCSF is computed. The lighthouse is set as a rigid body with the same displacement at each part. Taking the lighthouse as the target of observation to record the creep subsidence of structures. The calibrated parameters when $p = 100$ kPa and $q = 200$ kPa listed in Tables 2 and 3 are used in computation for the material ② and material ③ ($\rho_d = 1.45$ g/cm³); meanwhile, the calibrated parameters when $p = 400$ kPa and $q = 2,000$ skPa listed in Tables 2 and 3 are used for the material ④ ($\rho_d = 1.65$ g/cm³). The parameters of the modified KBM and HBM used in computation are all illustrated in Table 6.

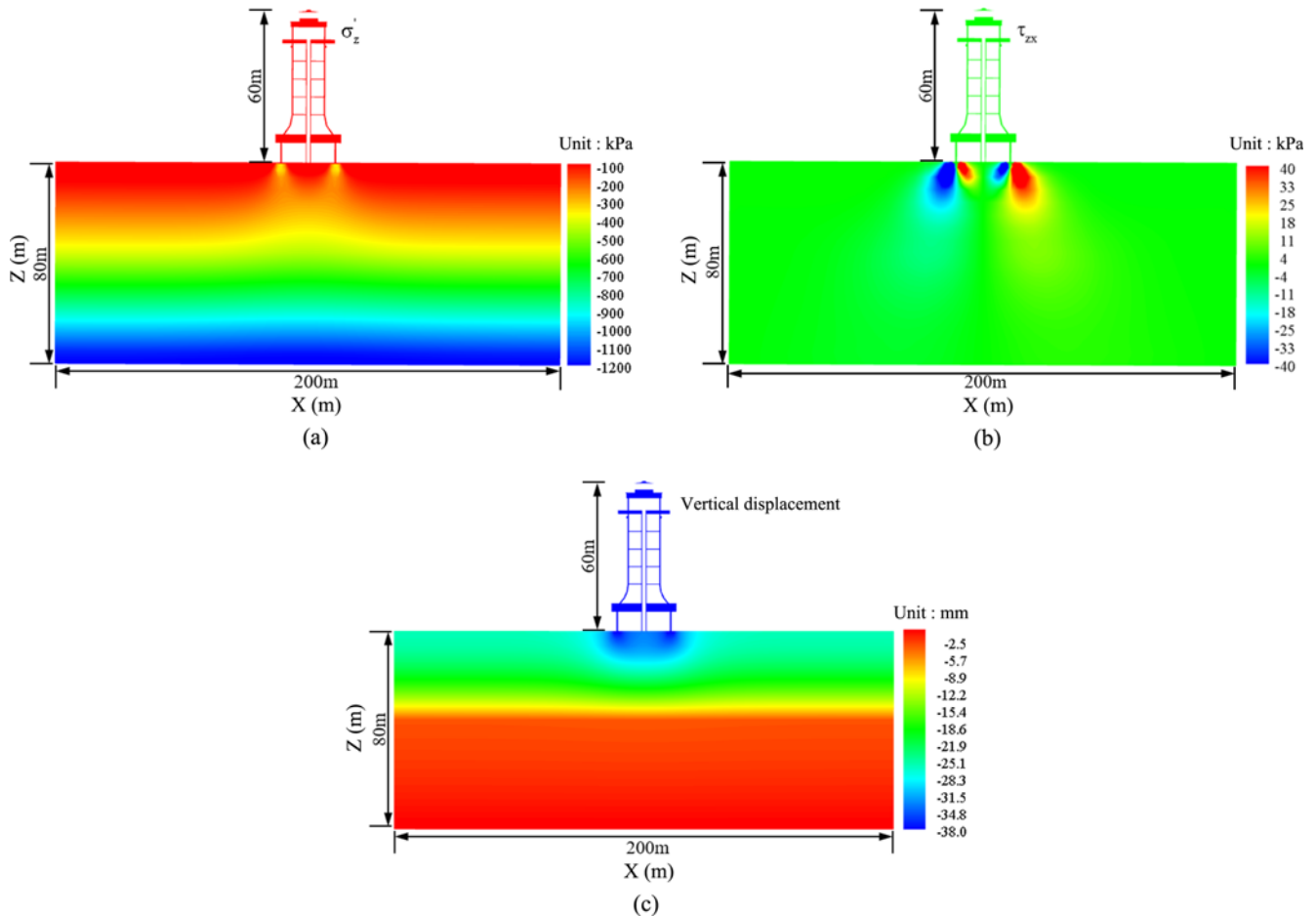
4.3 Analysis of Long-Term Settlement

4.3.1 Initial State

During the lighthouse foundation reclaiming and the construction of the lighthouse, the lighthouse foundation certainly undergoes

Table 6. Parameters of Modified KBM and HBM Adopted in Computation

	Materials	E_1 (MPa)	η_1 (GPa · min)	C (MPa)	β	K	m	n
Modified KBM	②	315	13.9	499	0.1474	0.562	1.139	0.449
	③	315	13.9	499	0.1474	0.562	1.139	0.449
	④	1,390	196	1,950	0.1963	0.445	1.1006	0.45
	Materials	E_1 (MPa)	η_1 (GPa · min)	A (GPa)	B	K	m	n
Modified HBM	②	274	624	4.6	0.0343	0.562	1.139	0.449
	③	274	624	4.6	0.0343	0.562	1.139	0.449
	④	470	1,590	24.2	0.0237	0.445	1.1006	0.45

**Fig. 6.** Distribution of σ'_z , τ_{zx} and U_z in the Initial State before Creeping: (a) Vertical Effective Stress σ'_z , (b) Shear Stress τ_{zx} , (c) Vertical Displacement U_z

an elastoplastic deformation process under their own weight loading. Finally a new equilibrium state will be reached. Only based on this new state, the long-term creep subsidence of the lighthouse can be analyzed. In computation, the static solver in ABAQUS is used to determine the initial deformation and initial stress in the foundation, as well as the initial subsidence of the lighthouse. In this analysis step, the modified KBM or HBM are also used. Due to the fact that $t = 0$ at the initial time, there is only the time-independent elasto-plastic deformation in the foundation according to the Eqs. (5) and (6). Also due to the fact

that there is no pore water is considered in the foundation, there is no the seepage and pore pressure dissipation process. As a consequence, there is no the consolidation process in the foundation when determining this initial condition.

Figure 6(a) illustrates the vertical effective stress σ'_z distribution at the initial state in the lighthouse and RCCSF. Because of the compression of the lighthouse gravity, σ'_z in the foundation below the structure is greater than that in the zone away from the structure. σ'_z in the zone away from the lighthouse is layered. It is indicated that the effect of the lighthouse gravity on σ'_z is

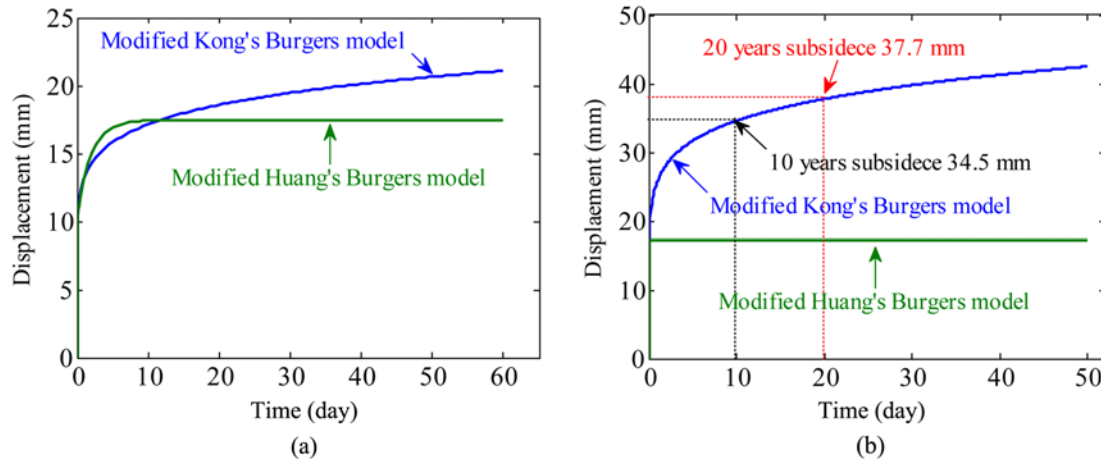


Fig. 7. The Time-Settlement Curve of the Lighthouse Constructed on the RCCSF: (a) 60 Days, (b) 50 Years (Note: The initial elastoplastic strain has been excluded.)

constrained in the zone near the lighthouse. σ'_z below the lighthouse in its foundation reaches 400 kPa. Fig. 6(b) demonstrates the distribution of shear stress τ_{zx} in the foundation. It can be seen that there are two concentration zone for τ_{zx} in the foundation around the lighthouse. The maximum τ_{zx} is about 100 kPa. Fig. 6(c) shows the distribution of the vertical displacement U_z at initial state in the calcareous sand foundation. It can be seen that the lighthouse has subsided downward about 3.8 cm before creeping.

4.3.2 Creep Process Analysis

Figures 7(a) and 7(b) illustrate the time-dependent settlement curve of the lighthouse (the initial elastoplastic strain is not included), respectively. Fig. 7(a) shows that the creep process of the lighthouse within 60-days determined by the modified KBM and HBM. The creep settlement of the lighthouse determined by the modified HBM is greater than that determined by the modified KBM within the first 10 days. However, the long-term creep of the lighthouse determined by the modified HBM becomes converged thereafter, and is always kept as 17.2 mm. Meanwhile, the long-term subsidence of the lighthouse determined by the modified KBM always increases with time gradually.

Figure 7(b) shows the computational results of the lighthouse subsidence in the future 50 years. The long-term subsidence of the lighthouse determined by the modified HBM is always kept as 17.2 mm. However, the settlement determined by the modified KBM always increases slowly during 50-years. But the increasing rate gradually becomes slow. The long-term post-construction creep subsidence of the lighthouse determined by the modified KBM is 34.5 mm in future 10 years, 37.5 mm in future 20 years, and 42.5 mm in future 50 years, respectively.

It can be concluded that the creep subsidence of the lighthouse constructed on the RCCSF in SCS determined by the modified KBM and HBM both are not great. The national design code of building foundation released by the Ministry of Housing and Urban-Rural Development of China (GB 50007-2001, 2011)

requires that the post-construction subsidence of a highrise structure with simple shape must be limited under 200 mm. Therefore, the creep subsidence of the lighthouse constructed on the RCCSF in the SCS meets the requirement stipulated by China National Code GB 50007-2011.

The model parameters of the modified KBM proposed in this study for CCS have been successfully calibrated utilizing the experimental results given by Cao and Ye (2019). As we know, the creep of materials generally is a gradually cumulative behavior. However, the triaxial creep tests are usually terminated based on an artificial standard, when the incremental deformation of a specimen in one day is less than 0.005 mm, a creep test will be terminated in this study. However, the creep strain of the specimen actually may has not developed fully at this moment. Therefore, it is impossible for us to get the complete test results of the creep process through some creep tests in laboratory. Only partial data of the creep process within several weeks or months could be recorded. As a consequence, it leads to some uncertainty when mathematical fitting is adopted to determine the model parameters of modified KBM and HBM proposed in this study.

As illustrated by Eqs. (5) and (6) that the modified KBM is not converged with time; meanwhile, the modified HBM is converged with time. The truth is that, it is difficult for us to exactly be aware of that the creep process of the CCS is converged or un-converged, because a complete creep experiment could need to be conducted for decades in which creep strain could fully developed. Based on this consideration and the convergence or non-convergence characteristics of the modified KBM and HBM, it is suggested that the settlement determined by the modified KBM can be treated as the upper limit; at mean time, the settlement determined by the modified HBM can be treated as the lower limit, when the subsidence of the lighthouse need to be numerically predicted. Therefore, the determined creep subsidence of the lighthouse is no longer a fixed value, but in a range. Finally, the settlement of the lighthouse constructed on the RCCSF in the SCS is predicted in the range of 17.2 to 34.5 mm at 10 years,

17.2 to 37.7 mm at 20 years and 17.2 to 42.5 mm at 50 years, respectively.

4.3.3 Sensitivity Analysis of Model Parameters

In order to further understand the influences of model parameters on the predicted creep subsidence of the lighthouse, sensitivity analysis is conducted for the model parameters here. The model parameters in this sensitivity study utilized in computation are determined based on the orthogonality theory. The theory is that one of the parameters is assigned as 5 different values; at the meantime, the other parameters will be kept invariable when this one model parameter's sensitivity is studied.

Due to the modified KBM is an un-converged model, only the sensitivity of the model parameter E_1 , η_1 , C and β which appear in the time-dependent terms in Eq. (5) of the modified KBM are examined here. Additionally, due to the fact that the reclaimed calcareous sand layer (labelled as material ② and ③ in analysis) is relatively loose ($\rho_d = 1.45 \text{ g/cm}^3$) compared with the its underlying original calcareous coral sand layer ($\rho_d = 1.65 \text{ g/cm}^3$, labelled as material ④ in analysis), the creep subsidence of the lighthouse is

mainly attributed to the creep behavior of the reclaimed loose CCS layer. Therefore, only the model parameters of the reclaimed loose CCS layer are involved in this sensitivity analysis. The parameter values of material ② and ③ listed in Table 6 are assigned as the standard values in this section. The model parameters of the modified KBM chosen for the sensitivity analysis have been listed in Table 7, in which the standard values have been labelled as the blue bold characters. Finally, the 50-years creep subsidence of the lighthouse is chosen as the representative to explore the sensitivity of the predicted subsidence to the model parameters of

Table 7. Model Parameters of Material ② and ③ for the Modified KBM in Sensitivity Analysis

	E_1/MPa	$\eta_1/\text{GPa}\cdot\text{min}$	C/MPa	β
	115	7.9	299	0.1074
Modified KBM	215	10.9	399	0.1274
	315	13.9	499	0.1474
	415	16.9	599	0.1674
	515	19.9	699	0.1874

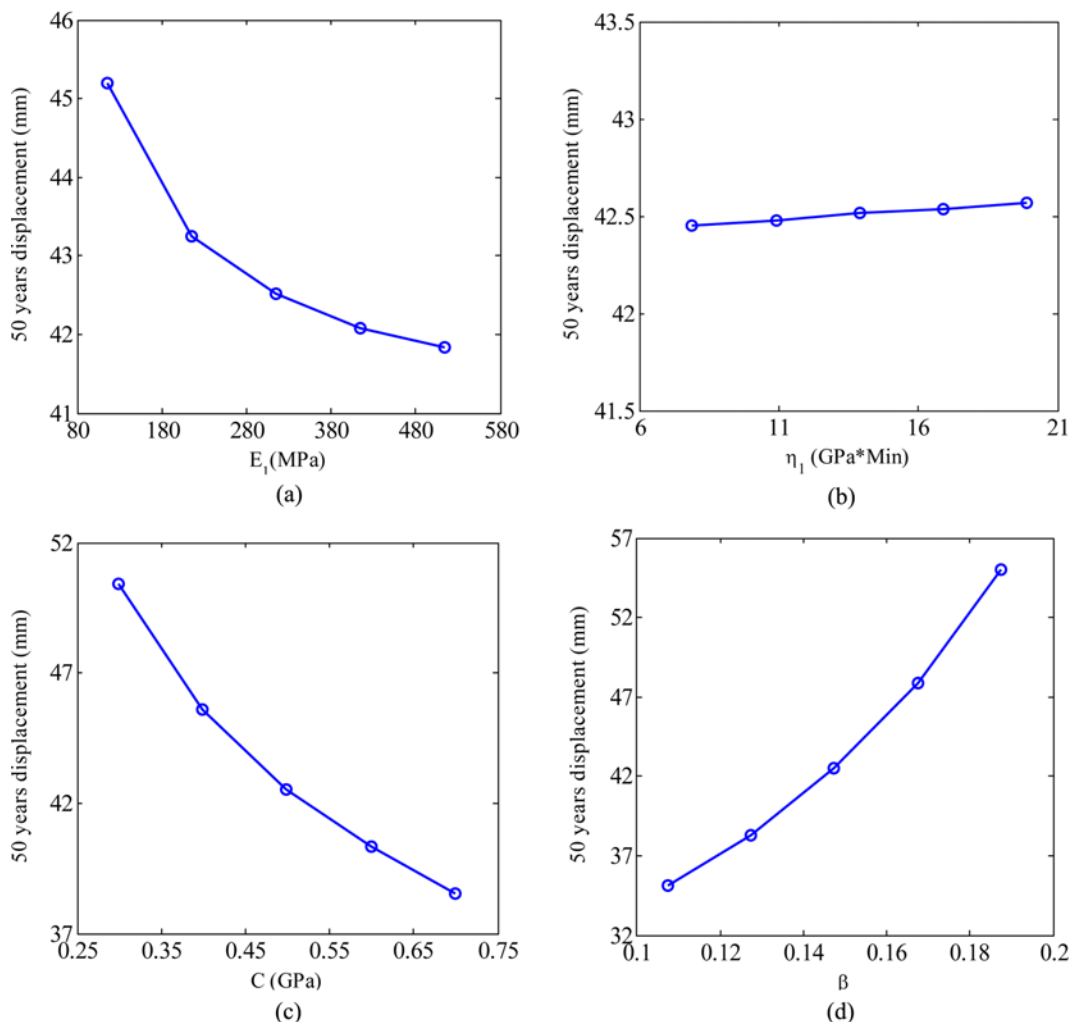


Fig. 8. The Sensitivity of the Predicted Creep Subsidence of the Lighthouse to the Model Parameters if the Modified KBM Is Adopted: (a) The Sensitivity of E_1 , (b) The Sensitivity of η_1 , (c) The Sensitivity of C , (d) The Sensitivity of β

the un-converged modified KBM.

Figure 8 shows that the parameter η_1 of material ② and ③ increases from 7.9 GPa·min to 19.9 GPa·min, but the 50-years creep subsidence of the lighthouse almost remains unchanged. Therefore, the predicted result is not sensitive to η_1 of material ② and ③. When the parameter C of material ② and ③ changes from 0.299 GPa to 0.699 GPa by 133%, the lighthouse 50-years creep subsidence declines only by 23.6%. Therefore, the predicted subsidence is less sensitive to C of material ② and ③. As the parameter β of material ② and ③ grows from 0.1074 to 0.1874 by 74%, the creep subsidence of the lighthouse grows by 57% at the future 50 years, it can be concluded that the predicted creep subsidence is moderately sensitive to β of material ② and ③. The parameter E_1 grows from 115 MPa to 515 MPa by 347%, while the lighthouse 50-years creep subsidence reduces by 7.4%. Therefore, the predicted result is basically not sensitive to E_1 of the material ② and ③.

Overall, the predicted post-construction creep subsidence of the lighthouse constructed on the RCCSF in the SCS is moderately sensitive to β , less sensitive to C , and not sensitive to η_1 and E_1 . Therefore, more attention should be paid to appropriately calibrate the model parameter β of material according to experimental results if the modified KBM is utilized.

5. Conclusions

Taking the reclamation project in the South China Sea as the engineering background, the post-construction creep subsidence of an ocean lighthouse constructed on the RCCSF is numerically predicted in this study. Based on the contents presented, the following conclusions are obtained:

1. Two modified creep models, referred as HBM and KBM, respectively, have been proposed in this study according to laboratory test data.
2. The finite element implementation algorithm for the two modified creep models has been presented. Based on this algorithm, the two modified creep models are successfully implanted into the commercial platform ABAQUS through the developer interface UMAT subroutine. It builds a solid basis for the subsequent work to numerically predict the creep subsidence of the ocean lighthouse.
3. The two modified creep models incorporating ABAQUS have been validated adopting a series of laboratory triaxial creep test results. It is indicated that the two proposed creep models are reliable.
4. It is predicted by the numerical modeling that the post-construction creep subsidence of the lighthouse constructed on RCCSF in SCS in the future 50 years is in the range of 17.2 mm to 42.5 mm, satisfying the mandatory requirement (<200 mm) stipulated by the Chinese national design code of building foundation GB 50007-2011.
5. It is indicated by the sensitivity analysis that the predicted result is moderately sensitive to the parameter β in the modified KBM. It reminds us that more attention should

be paid when the sensitive model parameters are calibrated based on laboratory creep experimental results.

Acknowledgments

We sincerely thank the financial support from the project “Strategic Priority Research Program of the Chinese Academy of Sciences (XDA13010202)”, and the support from National Natural Science Foundation of China (51879257).

ORCID

Not Applicable

References

- Cao WG, Yang S, Zhang C (2017) A statistical damage constitutive model of rocks considering the variation of the elastic modulus. *Hydrogeology and Engineering Geology* 44(3):42-48, DOI: [10.16030/j.cnki.issn.1000-3665.2017.03.07](https://doi.org/10.16030/j.cnki.issn.1000-3665.2017.03.07) (in Chinese)
- Cao M, Ye JH (2019) Creep-stress-time four parameters mathematical model of calcareous sand in South China Sea. *Rock and Soil Mechanics* 40(5):1771-1777, DOI: [10.16285/j.rsm.2018.1267](https://doi.org/10.16285/j.rsm.2018.1267) (in Chinese)
- Di H, Zhou S, Xiao J, Gong QM, Luo Z (2016) Investigation of the long-term settlement of a cut-and-cover metro tunnel in a soft deposit. *Engineering Geology* 204:33-40, DOI: [10.1016/j.enggeo.2016.01.016](https://doi.org/10.1016/j.enggeo.2016.01.016)
- Dorfman JR, Faller AJ (1982) Jan burgers. *Physics Today* 35(1):84-85, DOI: [10.1063/1.2890021](https://doi.org/10.1063/1.2890021)
- Enomoto T, Koseki J, Tatsuoka F, Sato T (2016) Creep failure of natural gravelly soil and its simulation. *Geotechnique* 66(11):865-877, DOI: [10.1680/jgeot.15.P.144](https://doi.org/10.1680/jgeot.15.P.144)
- Fu KM, Huang XM (2008) The secondary development of modified burgers creep model based on ABAQUS general software. *Highway Engineering* 3:132-137 (in Chinese)
- GB 50007-2001 (2011) Code for design of building foundation. Ministry of Housing and Urban-Rural Development of China, Architecture & Building Press, Beijing, China (in Chinese)
- He LJ, Kong LW, Wu WJ, Cai Y (2011) A description of creep model for soft soil with fractional derivative. *Rock and Soil Mechanics* 32(S2):239-249, DOI: [10.16285/j.rsm.2011.s2.022](https://doi.org/10.16285/j.rsm.2011.s2.022) (in Chinese)
- Jiang L, Lin H (2010) Integrated analysis of SAR interferometric and geological data for investigating long-term reclamation settlement of Chek Lap Kok Airport, Hong Kong. *Engineering Geology* 110(3-4): 77-92, DOI: [10.1016/j.enggeo.2009.11.005](https://doi.org/10.1016/j.enggeo.2009.11.005)
- Liu CQ, Wang R, Wu XS (1999) Some problems for the tests of physical-mechanical properties of calcareous sand. *Chinese Journal of Rock Mechanics and Engineering* 18(2):91-94 (in Chinese)
- Lv Y, Li F, Liu Y W, Wang M Y (2017) Comparative study of coral sand and silica sand in creep under general stress states. *Canadian Geotechnical Journal* 54(11):1601-1611, DOI: [10.1139/cgj-2016-0295](https://doi.org/10.1139/cgj-2016-0295)
- Mesri G, Febres-Cordero E, Shields DR, Castro A (1981) Shear stress-strain-time behaviour of clays. *Geotechnique* 31(4):537-552, DOI: [10.1680/geot.1981.31.4.537](https://doi.org/10.1680/geot.1981.31.4.537)
- Murayama S (1983) Formulation of stress-strain-time behavior of soils under deviatoric stress condition. *Soils and Foundations* 23(2):43-57, DOI: [10.3208/sandf1972.23.2_43](https://doi.org/10.3208/sandf1972.23.2_43)
- Nishihara M (1952) Creep of shale and sandy-shale. *The Journal of the Geological Society of Japan* 58(683):373-377, DOI: [10.5575/](https://doi.org/10.5575/)

- [geosoc.58.373](#)
- Nishihara M (1958) Rheological properties of rocks I and II. *Doshisha Engineering Review* 8:85-115
- Pramthawee P, Jongpradist P, Sukkarak R (2017) Integration of creep into a modified hardening soil model for time-dependent analysis of a high rockfill dam. *Computer and Geotechnics* 91:104-116, DOI: [10.1016/j.compgeo.2017.07.008](#)
- Qiu J, Liu H, Lai J, Lai H P, Che JX (2018) Investigating the long-term settlement of a tunnel built over improved loessial foundation soil using jet grouting technique. *Journal of Performance of Constructed Facilities* 32(5):04018066, DOI: [10.1061/\(ASCE\)CF.1943-5509.0001155](#)
- Shahnazari H, Rezvani R (2013) Effective parameters for the particle breakage of calcareous sands: An experimental study. *Engineering Geology* 159:98-105, DOI: [10.1016/j.enggeo.2013.03.005](#)
- Shen SL, Wu HN, Cui YJ, Yin ZY (2014) Long-term settlement behaviour of metro tunnels in the soft deposits of Shanghai. *Tunnelling and Underground Space Technology* 40:309-323, DOI: [10.1016/j.tust.2013.10.013](#)
- Shi YJ, Li MG, Chen JJ, Wang JH (2018) Long-term settlement behavior of a highway in land subsidence area. *Journal of Performance of Constructed Facilities* 32(5):04018063, DOI: [10.1061/\(ASCE\)CF.1943-5509.0001195](#)
- Singh A, Mitchell JK (1968) General stress-strain-time function for soils. *Journal of the Soil Mechanics and Foundations Division* 94(1):21-46, DOI: [10.1016/0022-4898\(68\)90146-8](#)
- Wang XZ, Wang R, Meng QS, Liu XP (2009) Study of plate load test of calcareous sand. *Rock and Soil Mechanics* 30(01):147-151, DOI: [10.16285/j.rsm.2009.01.039](#) (in Chinese)
- Wongsaroj J, Soga K, Mair RJ (2013) Tunnelling-induced consolidation settlements in London Clay. *Geotechnique* 63(13):1103, DOI: [10.1680/geot.12.P.126](#)
- Yao YP, Wang K, Wang ND, Zhang QL (2019) Prediction method on long-term settlement of high-speed railway subgrade under the influence of near-load. *Chinese Journal of Geotechnical Engineering* 41(04):625-630
- Ye JH, Cao M (2019) Preliminary study on the creep characteristics of calcareous sand from reclaimed coral reef islands in South China Sea. *Chinese Journal of Rock Mechanics and Engineering* 38(06):1242-1251, DOI: [10.13722/j.cnki.jrme.2018.0695](#) (in Chinese)
- Zhang YC, Gao F, Lu GS, Ma C, Zhao Y (2018a) Numerical simulation of high fill foundation settlement based on creep test of loess. *Science Technology and Engineering* 18(30):220-227
- Zhang Y, Yu DW, Ye JH (2018b) Study on measurement methodology of tensile elastic modulus of rock materials. *Rock and Soil Mechanics* 39(6):2295-2303, DOI: [10.16285/j.rsm.2017.2192](#) (in Chinese)
- Zhang CC, Zhu HH, Shi B, Fatahi B (2018c) A long term evaluation of circular mat foundations on clay deposits using fractional derivatives. *Computer and Geotechnics* 94:72-82, DOI: [10.1016/j.compgeo.2017.08.018](#)